Time-resolved measurement of spin-wave spectra in CoO capped [Co(t)/Pt(7Å)]$_{n-1}$ Co(t) multilayer systems

S. Pal, B. Rana, S. Saha, R. Mandal, O. Hellwig, J. Romero-Vivas, S. Mamica, J. W. Klos, M. Mruczkiewicz, M. L. Sokolovskyy, M. Krawczyk, and A. Barman

Citation: Journal of Applied Physics **111**, 07C507 (2012);
View online: https://doi.org/10.1063/1.3672857
View Table of Contents: http://aip.scitation.org/toc/jap/111/7
Published by the American Institute of Physics

Time-resolved measurement of spin-wave spectra in CoO capped $[Co(t)/Pt(7Å)]_{n-1}$ Co(t) multilayer systems

S. Pal,[1] B. Rana,[1] S. Saha,[1] R. Mandal,[1] O. Hellwig,[2] J. Romero-Vivas,[3] S. Mamica,[3] J. W. Klos,[3] M. Mruczkiewicz,[3] M. L. Sokolovskyy,[3] M. Krawczyk,[3] and A. Barman[1,a)]
[1]*Department of Condensed Matter Physics and Material Sciences, S. N. Bose National Centre for Basic Sciences, Block JD, Sector III, Salt Lake, Kolkata 700 098, India*
[2]*San Jose Research Center, Hitachi Global Storage Technologies, 3403 Yerba Buena Rd., San Jose, California 95135, USA*
[3]*Faculty of Physics, A. Mickiewicz University, Umultowska 85, 61-614 Poznań, Poland*

(Presented 2 November 2011; received 23 September 2011; accepted 28 October 2011; published online 24 February 2012)

We present an all-optical time-resolved measurement of dipole-exchange spin wave spectra in a series of CoO capped $[Co(t)/Pt(7\ Å)]_{n-1}$ Co(t) multilayer systems, where the total Co moment ($n \times t$) is constant. In general, the spectra consist of two intense peaks and additional lower intensity peaks. The observed spin wave modes are modeled by a discrete dipole approximation. The frequency of the spin wave bands depends significantly upon the magnetic anisotropy and the lattice spacing between planes. Both symmetric and anti-symmetric modes are observed from the calculation of the spin-wave profiles across the multilayer in the out-of-plane direction. © *2012 American Institute of Physics*. [doi:10.1063/1.3672857]

Magnetic multilayers (MLs) with perpendicular magnetic anisotropy (PMA) have inspired technological progress within magnetic data storage,[1] spin transfer torque magnetic tunnel junctions,[2] and magnonic crystals.[3,4] New applications, such as in magnetic metamaterials with a negative refractive index in the high GHz frequency regimes using magnetic MLs have been theoretically predicted.[5] For many of these applications, exploration of rich spin wave bands in such MLs are desirable. There have been very few experimental efforts made of measuring the spin wave spectra in MLs with PMA by frequency and wave-vector domain techniques. Exchange dominated collective spin-wave excitations have been observed in Co/Pd MLs by Brillouin light scattering.[6] On the contrary, the spectra of standing spin waves have been detected by ferromagnetic resonance.[7] Theoretical investigations of spin waves in such MLs have been done by various methods including effective medium formulation,[8] and analytical methods including the Ruderman–Kittel–Kasuya–Yosida interaction[9] and discrete dipole approximation.[10]

Time-resolved measurements of the magnetization dynamics of Co/Pd and Co/Pt MLs with PMA have become a subject of recent interest.[11–14] However, those studies focused mainly upon the excitation and detection of the fundamental spin wave mode of the whole ML stack and the time-domain excitation and detection of the spin wave manifold remained unexplored. Here, we report on the all-optical excitation and detection of dipole-exchange spin waves in a series of CoO capped $[Co(t)/Pt(7\ Å)]_{n-1}Co(t)$ ML systems. The observed spin wave modes are reproduced by theoretical calculations based upon discrete dipole approximation (DDA).

A series of $[Co(t)/Pt(7\ Å)]_{n-1}$ Co(t) MLs with variable Co layer thickness (t) and number of bilayer repeats (n) were deposited by DC magnetron sputtering.[15] The product, $n \times t = 80$ Å was kept constant. The thickness of the top Co-layer was increased from t to $t + 12$ Å and then exposed to ambient air, thus yielding oxidation of the top ~12 Å of Co into ~15–20 Å of CoO for optional exchange biasing below room temperature.[16] All of the experiments reported here are performed at room temperature and the CoO layer can be considered paramagnetic with no exchange bias effect. However, the CoO top layer still introduces an asymmetry between the top and bottom of the Co/Pt ML. The Co layer thickness within the ML is varied from 0.2 nm ($n = 40$) to 0.8 nm ($n = 10$) in this experiment. The magnetic hysteresis loops were measured by the polar magneto-optical Kerr effect. The time-resolved magnetization dynamics were measured by a home built all-optical time-resolved magneto-optical Kerr effect (TR-MOKE) magnetometer, as described in detail elsewhere.[14] A bias magnetic field ($\boldsymbol{H}$) is applied at a small angle (~10°) to the surface normal of the sample during the dynamical measurements.

Figure 1(a) shows the polar magneto-optical Kerr effect loops for samples with $n \times t = 40 \times 0.2$, 13×0.6, and 10×0.8 nm, respectively. Figure 1(b) shows the experimental x-ray reflectivity data with the theoretical fit for the sample with $t = 0.8$ nm. The extracted layer thickness is very close to the nominal thickness and the average interface roughness is of the order of 0.05 nm. Figure 1(c) shows typical time-resolved reflectivity and Kerr rotation data and the corresponding fast Fourier transform (FFT) spectra from the ML with $t = 0.6$ nm at $H = 2.47$ kOe. The precessional dynamics appear as an oscillatory signal above the slowly decaying part of the time-resolved Kerr rotation after a fast demagnetization within the first 400 fs, and a fast remagnetization.

Figure 2 shows the bi-exponential background subtracted time-resolved Kerr rotation data and the

a)Electronic mail: abarman@bose.res.in.

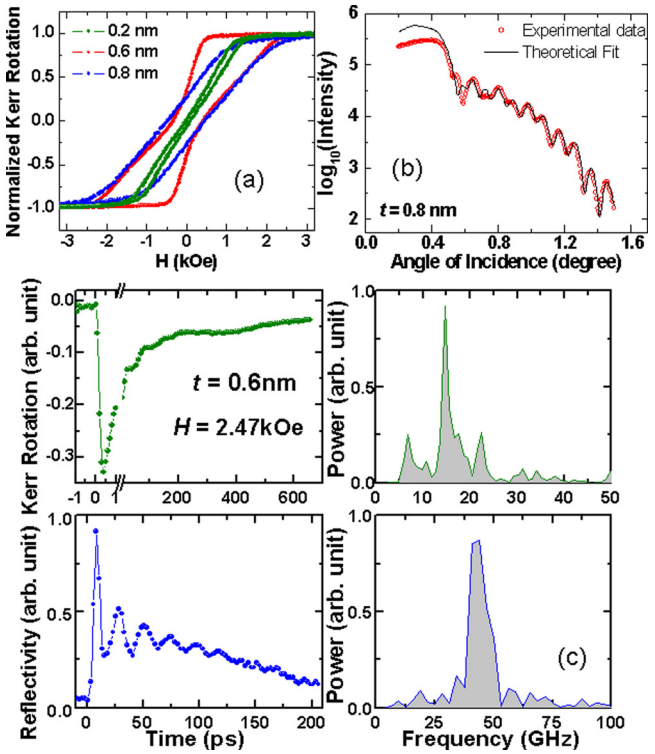

FIG. 1. (Color online) (a) Polar magneto-optical Kerr loops for a series of $[Co(t)/Pt(7\ Å)]_{n-1}$ Co(t) samples. (b) The experimental and fitted x-ray reflectivity results from the multilayer sample with $t = 0.8$ nm. (c) The time-resolved reflectivity and Kerr rotation data and the corresponding FFT spectra are shown for the ML with $t = 0.6$ nm at $H = 2.47$ kOe.

corresponding FFT spectra for the samples. In the FFT spectra for $t = 0.2$ nm, we observe two intense peaks below 10 GHz and small amplitude peaks above 20 GHz. For $t = 0.6$ nm, we observe a prominent peak followed by a shoulder below 10 GHz, a band of modes between 10 and 20 GHz, and a small amplitude band at around 30 GHz. For $t = 0.8$ nm, we observe large amplitude split modes below 10 GHz, a large amplitude broad band between 10 and 15 GHz, and two small amplitude narrow bands at around 20 and 30 GHz.

The aim of the theoretical modeling is twofold: (1) the verification of the hypothesis that standing waves formed

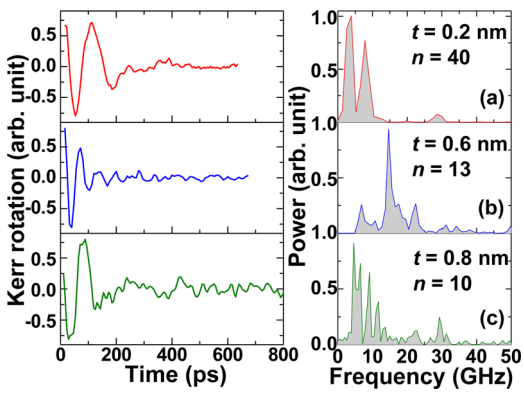

FIG. 2. (Color online) Time-resolved Kerr rotation data and the corresponding FFT spectra for $[Co(t)/Pt(7\ Å)]_{n-1}$ Co(t) multilayers with (a) $n \times t = 40 \times 0.2$ nm, (b) 13×0.6 nm and (c) 10×0.8 nm at $H = 2.47$ kOe.

across the $[Co(t)/Pt(7Å)]_{n-1}$ Co(t) ML can explain the multi-peak spectra observed in the TR-MOKE measurements, and (2) to establish the spin pinning at the surface of the ML introduced by the paramagnetic CoO layer on top of the ML. In order to do that, we considered a system of magnetic moments, μ_r, regularly disposed in sites, $\boldsymbol{r}$, of a sample consisting of stacks of planes with magnetic moments arranged on the two-dimensional crystallographic lattice points of a simple hexagonal crystal lattice (see Fig. 3(a)). Solely Co or Pt magnetic moments (μ_{Co} or μ_{Pt}) are present on each single plane, i.e., we assume sharp interfaces in our model. The 7 Å thick Pt layers are modeled by 3 Pt monolayers in all studied samples. The MLs with $t = 0.2$, 0.6, and 0.8 nm were modeled with 1, 3, and 4 monolayers of Co in each unit cell.

The spin-wave spectra were calculated in a linear approximation, without damping by numerically solving the Landau-Lifshitz equation on the discrete lattice—DDA method.[17] The analysis was limited only to the standing waves formed across the ML.[10,17] We considered the sample in a saturated state along the direction of the effective field. The approximate direction of the static magnetization was found from the standard equation with the assumption of a uniform thin film.[18] In the Co planes we assumed a magnetic moment of $1.8\mu_B$ (or $1.9\mu_B$ for one sample), while for the Pt planes a smaller induced magnetic moment (μ_{Pt}) due to the close proximity to the Co atoms was used.[19] All parameters used in the calculations are summarized in Table I.

The intensities of the standing wave (SW) lines measured in the TR-MOKE were compared with the relative intensities calculated according to the procedure described in Ref. 20. The anisotropy constant, magnetic moment induced on Pt, and the exchange integral between the Pt-Pt planes were changed to obtain agreement between the experimental and theoretical results; see Table I. Figure 3(b) shows the spectrum calculated for the ML with $n \times t = 13 \times 0.6$ nm at $H = 2.47$ kOe. We found good qualitative agreement with the experimental FFT spectrum, as shown in Fig. 2(b). A non-zero anisotropy equal to 3.9×10^5 J/m^3 limited to

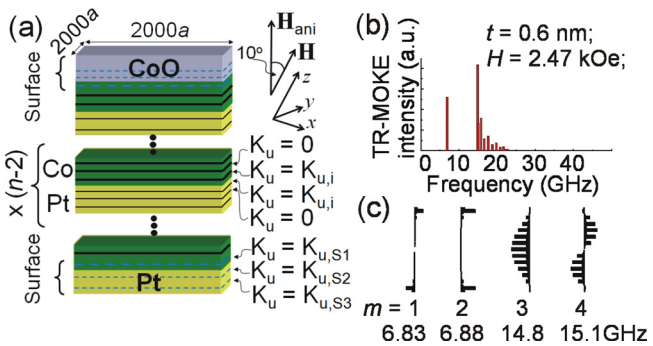

FIG. 3. (Color online) (a) Model structure of the Co/Pt ML film used in the calculations. The lateral sizes of the ML film are $2000a \times 2000a$, where $a = 2.29$ Å is the in-plane lattice constant. The bias magnetic field, $\boldsymbol{H}$, is rotated 10° from the surface normal of the film. The anisotropy constants on the surface layers ($K_{u,S1}$, $K_{u,S2}$, and $K_{u,S3}$) and at the interfaces ($K_{u,i}$) are different from zero. (b) TR-MOKE relative intensities calculated with the DDA method for the ML with $t = 0.6$ nm at $H = 2.47$ kOe. (c) The profiles of the SWs with low frequencies from the spectra shown in (b). Mode number, m, and the corresponding frequency of the mode are listed below.

TABLE I. Exchange integral ($J_{Pt\text{-}Pt}$), magnetic moments (μ_{Co}, μ_{Pt}), anisotropy constants at interfaces ($K_{u,i}$), the average anisotropy field (H_{ani}), and the anisotropy constant at external surfaces ($K_{u,S1}$, $K_{u,S2}$, $K_{u,S3}$, the same values on both surfaces) used for calculations of the SW spectra in $[Co(t)/Pt(7\ Å)]_{n\text{-}1}$ $Co(t)$ MLs. The values of $J_{Co\text{-}Co}$ and $J_{Co\text{-}Pt}$ were the same in all MLs and equal to 2.4×10^{-21} J.

MLs t (nm)	$J_{Pt\text{-}Pt}$ (10^{-21}J)	μ_{Co} (μ_B)	μ_{Pt} (μ_B)	$K_{u,i}$ (10^5 J/m^3)	H_{ani} (T)	$K_{u,S1}$ (10^5J/m^3)	$K_{u,S2}$ (10^5J/m^3)	$K_{u,S3}$ (10^5J/m^3)
0.2	0.086	1.9	0.18	1.78	0.71	1.78	0.712	0.0
0.6	0.200	1.8	0.27	3.9	0.36	1.86	1.86	−0.78
0.8	0.140	1.8	0.25	4.0	0.28	3.33	3.33	−0.80

planes at interfaces (see Fig. 3(a)) was used in the calculation. In order to separate the first mode from the frequency band, we had to assume different anisotropy values at the external surfaces of the ML. By surface layers we mean the last (first) layers with a non-zero magnetic moment, i.e., last (first) Co plane (S1) and two neighbor planes, S2 and S3 (in Fig. 3(a) marked by dashed lines). The corresponding values of the surface anisotropy constants are summarized in Table I. Here, we assumed the same anisotropy on the bottom and top surfaces of the ML.

The spectrum in Fig. 3(b) can be split into two groups of modes according to the profiles of the SWs presented in Fig. 3(c): (1) low frequency surface waves (antisymmetric and symmetric, at 6.83 and 6.88 GHz, respectively), and (2) the band of the bulk SWs (starting at 14.8 GHz). Changes of the anisotropy on the external surfaces results only in a shift of the surface modes.

The calculated SW spectra for the ML with $n \times t = 10 \times 0.8$ nm are shown in Figs. 4(a) and 4(b) with the fitted parameters shown in Table I. The two low frequency modes are almost degenerate in the calculations (5.36 GHz, Fig. 4(b)), while in the experiment two modes, at 4.6 and 6.5 GHz, are found. This is a result of the ideal symmetry assumed in the calculations, while in the real structure asymmetry between the top and bottom surfaces of the ML is present due to the presence of different materials; Pt on the bottom and CoO on the top. The introduction of the asymmetry will result in the splitting of the symmetric and antisymmetric modes. This is confirmed in Fig. 4(a) where the results of the calculations with different anisotropies on the top and bottom surfaces are shown. We assumed $K_{u,S1} = K_{u,S2}$ ($K_{u,S3}$) equal to 4.0×10^5 (-0.8×10^5) and 3.33×10^5 (-0.89×10^5) J/m^3 on the top and bottom surfaces of the multilayered structure, respectively.

Finally, we calculated the SW spectrum for the $[Co(2\ Å)/Pt(7\ Å)]_{n\text{-}1}$ $Co(2\ Å)$ ML as shown in Fig. 4(c). For such a small thickness of the Co layers it is expected to have a cluster formation at the interfaces. The first two peaks (with degenerate frequencies) are connected with surface excitations, as previously observed. The second broad peak consists of 38 modes, with frequencies lying in the range between 7.6 and 11.8 GHz. The width of the band indicates the strength of the interaction, i.e., narrowing of the band points to a decrease of the interaction between the magnetic moments in the multilayered structure. This explains the lower value of the exchange integral assumed in the calculations.

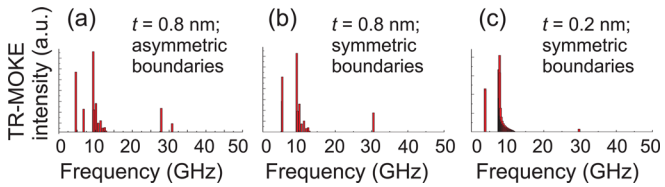

FIG. 4. (Color online) Relative intensities calculated with the DDA method for $[Co(t)/Pt(7\ Å)]_{n\text{-}1}$ $Co(t)$ ML with (a) $t = 0.8$ nm ($n = 10$) and asymmetric magnetic anisotropies at the surfaces, (b) $t = 0.8$ nm with symmetric surfaces, and (c) $t = 0.2$ nm ($n = 40$) with symmetric surfaces. The magnetic field assumed in the calculations was $H = 2.47$ kOe.

To conclude, we found good agreement between TR-MOKE measurements of MLs with PMA and a simple theoretical model used to calculate standing SW spectra in such PMA-MLs. The PMA field found is lower compared to those in the Co/Pd multilayers. The important aspect for modeling the low frequency part of the spectra is to include the external surfaces of the ML correctly. It means that this part of the spectra is affected by the substrate or the overlayer, roughness, cluster formation, or anisotropy distribution on the surfaces. The lines with higher frequencies are created by bulk excitations in the multilayered structure.

ACKNOWLEDGMENTS

We gratefully acknowledge the financial assistance from the Department of Science and Technology, Government of India (Grant Nos. INT/EC/CMS (24/233552) and SR/NM/NS-09/2007) and the European Community's Seventh Framework Programme (FP7/2007-2013) under Grant Agreement No. 233552 for the DYNAMAG project.

[1]T. Thomson *et al.*, Phys. Rev. Lett. **96**, 257204 (2006); O. Hellwig *et al.*, Appl. Phys. Lett. **90**, 162516 (2007).
[2]S. Mangin *et al.*, Nature Mater. **5**, 210 (2006).
[3]S. A. Nikitov *et al.*, J. Magn. Magn. Mater. **236**, 320 (2001).
[4]M. Krawczyk and H. Puszkarski, Phys. Rev. B **77**, 054437 (2008).
[5]R. V. Mikhaylovskiy *et al.*, Phys. Rev. B **82**, 195446 (2010).
[6]B. Hillebrands *et al.*, Phys. Rev. B **42**, 6839 (1990).
[7]R. S. Iskhakov *et al.*, JETP Lett. **83**, 28 (2006).
[8]R. L. Stamps and R. E. Camley, Phys. Rev. B **54**, 15200 (1996).
[9]J. T. Haraldsen and R. S. Fishman, J. Phys.: Cond. Matt. **22**, 186002 (2010).
[10]M. Krawczyk *et al.*, J. Appl. Phys. **109**, 113903 (2011).
[11]A. Barman *et al.*, J. Appl. Phys. **101**, 09D102 (2007).
[12]S. Mizukami *et al.*, Appl. Phys. Lett. **96**, 152502 (2010).
[13]Z. Liu *et al.*, J. Magn. Magn. Mater. **323**, 1623 (2011).
[14]S. Pal *et al.*, Appl. Phys. Lett. **98**, 082501 (2011).
[15]O. Hellwig *et al.*, Appl. Phys. Lett. **95**, 232505 (2009).
[16]O. Hellwig *et al.*, Phys. Rev. B **65**, 144418 (2002).
[17]H. Puszkarski *et al.*, J. Appl. Phys. **101**, 024326 (2007).
[18]A. G. Gurevich and G. A. Melkov, *Magnetization Oscillations and Waves* (CRC, Boca Raton, 1996).
[19]A. Kashyap *et al.*, J. Appl. Phys. **95**, 7480 (2004).
[20]J. Hamrle *et al.*, J. Phys. D: Appl. Phys. **43**, 325004 (2010).